Report

Cell Reports

Activity-Dependent Plasticity of Spike Pauses in Cerebellar Purkinje Cells

Graphical Abstract

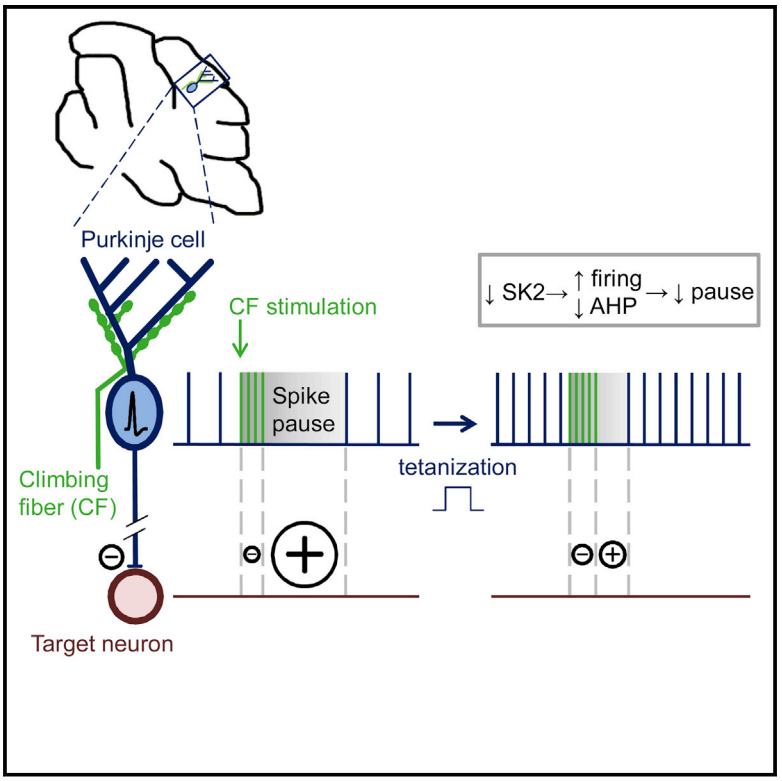

Authors

Giorgio Grasselli, Qionger He, Vivian Wan, John P. Adelman, Gen Ohtsuki, Christian Hansel

Correspondence

chansel@bsd.uchicago.edu

In Brief

Grasselli et al. find that in cerebellar Purkinje cells the pauses following spike bursts can be intrinsically modulated in an activity-triggered, SK2-channel-dependent way, altering the spike output pattern of these neurons. These findings show that the output of the cerebellar cortex is efficiently adjusted by an entirely non-synaptic plasticity mechanism.

Highlights

- Purkinje cell intrinsic plasticity is activity dependent, and entirely non-synaptic
- Repeated depolarization enhances spike firing and shortens pauses following bursts
- Pause plasticity is mediated by SK2 channel downregulation (apamin; $SK2^{-/-}$ mice)
- Pause plasticity is a phenomenon that can be separated from spike rate changes

Grasselli et al., 2016, Cell Reports *14*, 2546–2553
March 22, 2016
http://dx.doi.org/10.1016/j.celrep.2016.02.054

OPEN ACCESS
CellPress

Cell Reports
Report

Activity-Dependent Plasticity of Spike Pauses in Cerebellar Purkinje Cells

Giorgio Grasselli,[1] Qionger He,[1,5] Vivian Wan,[1] John P. Adelman,[2] Gen Ohtsuki,[3,4] and Christian Hansel[1,*]
[1]Department of Neurobiology, University of Chicago, Chicago, IL 60637, USA
[2]Vollum Institute, Oregon Health & Science University, Portland, OR 97239, USA
[3]Department of Biophysics, Graduate School of Science, Kyoto University, Kyoto 606-8502, Japan
[4]The Habuki Center, Kyoto University, Kyoto 606-8302, Japan
[5]Present address: Department of Physiology, Northwestern University, Chicago, IL 60611, USA
*Correspondence: chansel@bsd.uchicago.edu
http://dx.doi.org/10.1016/j.celrep.2016.02.054

SUMMARY

The plasticity of intrinsic excitability has been described in several types of neurons, but the significance of non-synaptic mechanisms in brain plasticity and learning remains elusive. Cerebellar Purkinje cells are inhibitory neurons that spontaneously fire action potentials at high frequencies and regulate activity in their target cells in the cerebellar nuclei by generating a characteristic spike burst-pause sequence upon synaptic activation. Using patch-clamp recordings from mouse Purkinje cells, we find that depolarization-triggered intrinsic plasticity enhances spike firing and shortens the duration of spike pauses. Pause plasticity is absent from mice lacking SK2-type potassium channels ($SK2^{-/-}$ mice) and in occlusion experiments using the SK channel blocker apamin, while apamin wash-in mimics pause reduction. Our findings demonstrate that spike pauses can be regulated through an activity-dependent, exclusively non-synaptic, SK2 channel-dependent mechanism and suggest that pause plasticity—by altering the Purkinje cell output—may be crucial to cerebellar information storage and learning.

INTRODUCTION

Current learning theories suggest that information storage in brain circuits results from activity-dependent changes in synaptic weight, such as in long-term potentiation (LTP) and depression (LTD), complemented by forms of non-synaptic (intrinsic) plasticity (Hansel et al., 2001; Daoudal and Debanne, 2003; Zhang and Linden, 2003; Magee and Johnston, 2005). It remains unknown, however, whether intrinsic plasticity might play a more significant role in the formation of memory engrams independent from its synaptic counterparts. This possibility might be particularly relevant for types of neurons that tonically fire action potentials, and whose spike patterns are to a significant extent shaped by intrinsic conductances.

Cerebellar Purkinje cells provide an interesting case to study consequences of intrinsic modulation for the generation of characteristic spike patterns, because activity-dependent intrinsic plasticity has been observed in these neurons in vitro and in vivo (Schreurs et al., 1998; Belmeguenai et al., 2010; Ohtsuki et al., 2012). Moreover, changes in Purkinje cell excitability have been described subsequent to motor learning (Schreurs et al., 1998), pointing toward a possible causal relationship between altered intrinsic excitability and learning. Purkinje cells are fast-spiking inhibitory projection neurons that spontaneously fire largely intrinsically generated action potentials at frequencies up to ~150 Hz (mean 38.8 Hz, in vitro [Häusser and Clark, 1997]; for review, see Simpson et al., 1996). A characteristic response pattern of these neurons to excitatory synaptic activity—at both parallel fiber (PF) and climbing fiber (CF) synapses—consists of a burst followed by a pause in spike firing (Granit and Phillips, 1956; Bell and Grimm, 1969; Bloedel and Roberts, 1971). In the target neurons in the cerebellar nuclei (CbN), this Purkinje cell output pattern translates into intensified inhibition followed by rebound currents and enhanced spike firing (Zheng and Raman, 2010).

Pauses following CF-evoked complex spikes and the underlying afterhyperpolarization (AHP), respectively, have been particularly well studied and result from recruitment of inhibitory interneurons by their CF inputs (Mathews et al., 2012), and from activation of calcium-dependent SK-type K^+ channels (Kakizawa et al., 2007). We have previously demonstrated that SK2 channel downregulation (Purkinje cells only express the SK2 isoform; Cingolani et al., 2002) mediates the increased spike activity in Purkinje cell intrinsic plasticity (Belmeguenai et al., 2010). Here, we address the question of whether spike pauses are modulated in an activity-dependent way, and use SK2 null mice ($SK2^{-/-}$) as well as selective inhibitors of calcium-dependent K^+ channels to examine the underlying cellular mechanism.

RESULTS

Intrinsic Plasticity Requires the Presence of Functional SK2 Channels

We performed whole-cell patch-clamp recordings from Purkinje cells in cerebellar slices obtained from P20-35 $SK2^{-/-}$ and wild-type (WT) mice at near-physiological temperature (32°C–34°C)

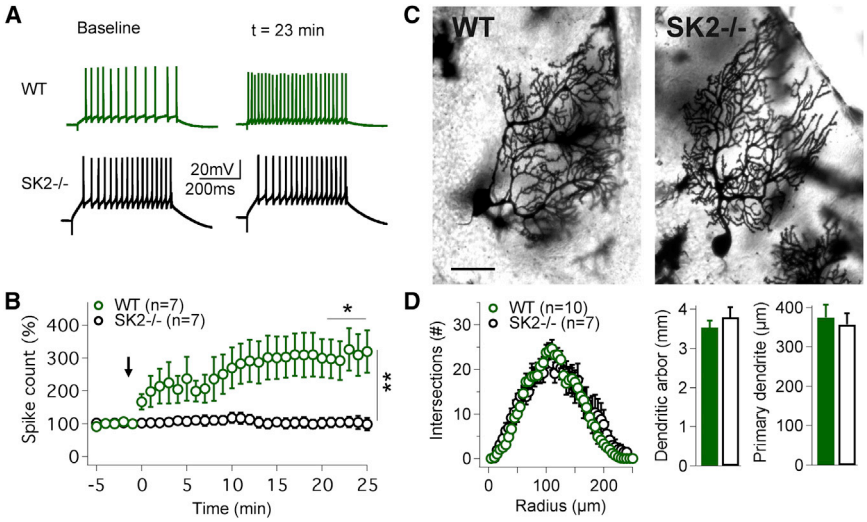

Figure 1. Intrinsic Plasticity Is Absent from SK2$^{-/-}$ Mice

(A) Top traces: in WT mice an increase in the spike count is triggered by a 5 Hz injection of depolarizing currents. Bottom traces: no excitability change is seen in SK2$^{-/-}$ Purkinje cells.

(B) Time graph showing that intrinsic plasticity is triggered in WT (n = 7), but not in SK2$^{-/-}$ Purkinje cells (n = 7). The arrow indicates the time point of tetanization.

(C) Golgi staining of Purkinje cells in WT (left) and SK2$^{-/-}$ mice (right). Scale bar, 50 μm.

(D) WT (n = 10) and SK2$^{-/-}$ Purkinje cells (n = 7) did not differ in dendritic complexity (Sholl analysis; left), the cumulative length of the dendrite (middle), or the length of the primary dendrite (right).

Values are shown as mean ± SEM. *p < 0.05; **p < 0.01.

to assess intrinsic plasticity in the absence of SK2 channels. During the test periods before and after tetanization, intrinsic excitability was measured by counting the number of spikes evoked by constant depolarizing current pulses (500 ms; 100–200 pA). For tetanization, repeated injection of depolarizing pulses was applied ("IP protocol": 5 Hz, 3 s; pulses: 100 ms/100–200 pA; Belmeguenai et al., 2010), which triggered an increase in the spike count in WT (305.3% ± 61.5%; t = 20–24 min; n = 7; p = 0.0268), but not in SK2$^{-/-}$ Purkinje cells (102.4% ± 14.9%; n = 7; p = 0.8752; difference between groups: p = 0.0021; Figures 1A and 1B), showing that SK2 channels are needed for intrinsic plasticity. To determine whether the absence of intrinsic plasticity in SK2$^{-/-}$ Purkinje cells might be due to cellular malformations, we performed Golgi staining and analyzed the morphology of the dendrite. We did not observe differences in the complexity of dendritic branching (Sholl analysis), in the cumulative length of the dendritic arbor (WT: 3.53 ± 0.17 mm; n = 10; SK2$^{-/-}$: 3.80 ± 0.25 mm; n = 7; p = 0.38), or the length of the primary dendrite (WT: 374.5 ± 32.2 μm; n = 10; SK2$^{-/-}$: 356.5 ± 28.0 μm; n = 7; p = 0.48; Figures 1C and 1D). These findings show that the absence of intrinsic plasticity from SK2$^{-/-}$ mice is not due to morphological alterations that might affect the membrane surface area or dendritic integration properties.

Pause Plasticity Is Activity Dependent and Mediated by SK2 Channel Downregulation

As SK2 channels contribute to the AHP following spike bursts (Kakizawa et al., 2007), we addressed the question whether spike pauses, which result from the underlying AHP, are modulated by intrinsic plasticity. Pauses are reliably observed following CF-evoked complex spikes (Simpson et al., 1996) and determine the shape of spike firing patterns in both Purkinje cells and their CbN target cells (Zheng and Raman, 2010). Thus, pause changes can be predicted to have a strong impact on cerebellar signaling.

To monitor complex spike pauses, Purkinje cells were first prevented from spike firing by the injection of negative bias currents. We then injected depolarizing current pulses (150–700 pA; 1 s) to mimic tonic spike firing (30–90 Hz range), and stimulated the CF input to elicit a complex spike (Figure 2A). The spike frequency and pause duration were typically adjusted and stabilized for about 10–15 min before baseline recording. To compensate for possible "wash-out" effects that might result from this delay, we modified the IP protocol to yield enhanced and prolonged depolarization (5 Hz, 7–8 s; pulses: 100 ms/500–700 pA). Application of this updated IP protocol caused a mild, but significant, increase in spike frequency (114.5% ± 3.6%; n = 14; p = 0.0007; Figure S1A). A reduction in the duration of the complex spike pause was seen in the tetanized group (to 81.4% ± 4.7%; t = 19–25 min; n = 14; p = 0.0059; Figure 2B; see also Figures 3E and 3F), but not in control recordings in the absence of tetanization (106.7% ± 4.4%; n = 8; p = 0.1192; Figure 2B). The pause changes in the tetanized and control group differed significantly from each other (p = 0.0041; Mann-Whitney U test). To examine a possible role of SK2 channels in pause plasticity, we repeated the experiment in SK2$^{-/-}$ mice. In these mice, application of the IP protocol did not shorten the pauses (97.7% ± 4.2%; n = 6; p = 0.5704; Figure 2C), suggesting that functional SK2 channels are needed for pause plasticity (for spike frequency measures in the control and SK2$^{-/-}$ groups, see Figure S1). To further study the involvement of SK channels in pause plasticity, we bath-applied the SK channel antagonist apamin (10 nM). Upon apamin wash-in, the pause was significantly shortened (49.9% ± 6.7%; n = 6; p = 0.0049; Figure 2D), while no reduction was seen in occlusion experiments, in which the IP protocol was applied when apamin (10 nM) was present in the bath (105.2% ± 13.4%; n = 6; p = 0.5354; Figure 2E). These data suggest that pause plasticity results from SK2 channel downregulation. It has previously been shown that large-conductance calcium-activated BK-type K^+ channels contribute to AHPs following calcium spikes in Purkinje cells (Edgerton and Reinhart, 2003). To examine whether BK channels are activated during complex spike pauses, we bath-applied the BK channel blocker paxillin (1 μM), while apamin (10 nM) was continuously present in the bath. Paxillin indeed enhanced the spike rate (171.7% ± 23.3%; n = 6; p = 0.0091) and shortened the pause

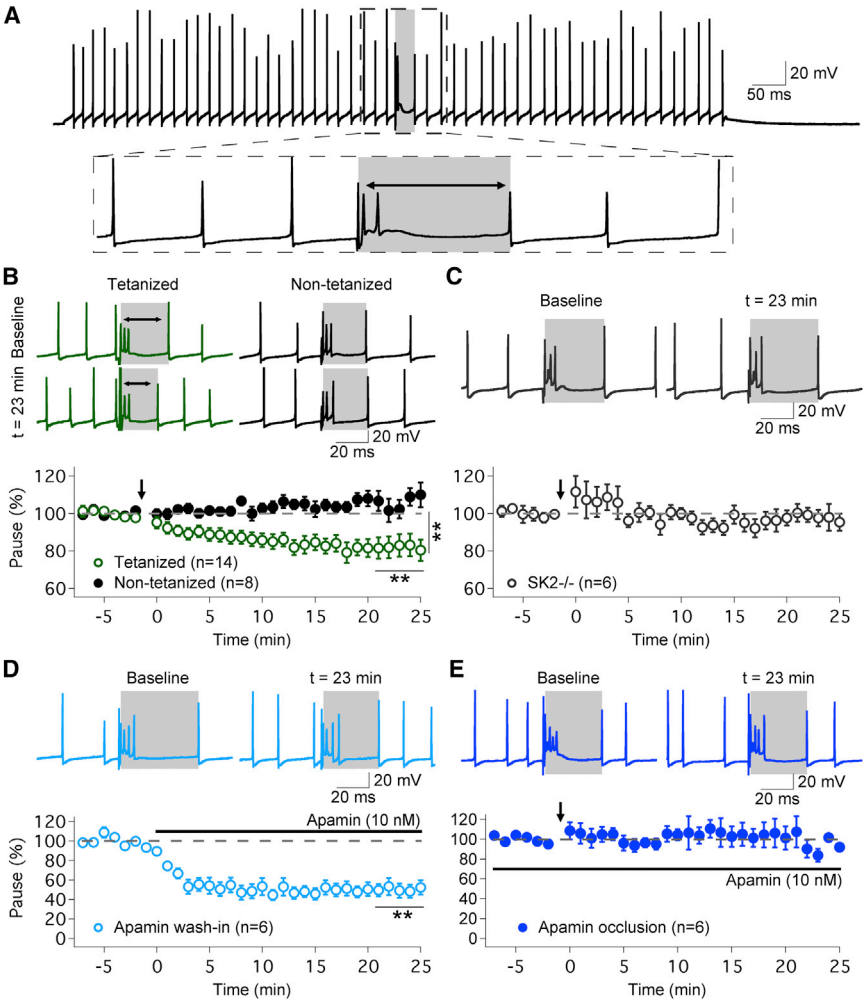

Figure 2. Plasticity of Complex Spike Pauses Is Mediated by SK2 Channel Downregulation

(A) Typical trace showing simple spike firing evoked by depolarizing current injection and a complex spike triggered by CF stimulation. The pause is measured as the interval between the complex spike onset and the next subsequent simple spike (gray area).

(B) Top: typical traces (green) show that 5 Hz injection of depolarizing currents causes a shortening of the spike pause. In contrast, pause duration remains stable in control recordings (black traces). Bottom: time graph showing that the IP protocol shortens the pause duration (n = 14), while the pause remains unaltered in non-tetanized cells (n = 8).

(C) In SK2$^{-/-}$ Purkinje cells, no pause plasticity is observed (n = 6).

(D) Wash-in of the SK channel inhibitor apamin (10 nM) shortens the pause duration (n = 6).

(E) The IP protocol does not trigger pause plasticity in the presence of apamin (10 nM) in the bath (n = 6). Arrows indicate the time point of tetanization.

Values are shown as mean ± SEM. **p < 0.01.

(71.8% ± 7.7%; n = 6; p = 0.0437; Figure S2). No change in spike frequency (99.3% ± 3.3%; n = 5; p = 0.7069) or pause length (99.1% ± 1.5%; n = 5; p = 0.5319; Figure S2) was observed when the blocker of intermediate-conductance, calcium-activated IK-type K^+ channels (Engbers et al., 2012), TRAM-34 (200 nM) was bath-applied. Thus, while both BK and SK2 channels contribute to the generation of pauses, the recordings from SK2$^{-/-}$ mice, complemented by the apamin experiments, suggest that SK2 channel downregulation is sufficient to explain pause plasticity.

Pause Plasticity: Contributions from a Reduction in the Complex Spike AHP and an Increase in Spike Firing

To describe the consequences of intrinsic plasticity for the Purkinje cell simple spike output, we plotted the distribution of interspike intervals (ISIs) before and after tetanization (Figure 3A). Only ISIs following complex spikes were included in this analysis to specifically assess how intrinsic plasticity modulates the spike pattern generated by CF stimulation. Application of the IP protocol significantly shifted the distribution curve toward shorter ISIs (n = 14; p = 0.008; Wilcoxon test on median values; Figure 3A). The plot reflects both the general increase in spike rate (shift in the peak) and the shortening of spike pauses. The latter effect is evident from a shortening of the right tail of the distribution curve (rescaled to align to the peaks; Kolmogorov-Smirnov test; p < 0.01; Figure 3C; see the Supplemental Information for details), and is supported by an increase in kurtosis values (“peakedness”; Figure 3B; p = 0.009). In addition, the largest ISI values (as a measure of the extension of the tails of the distribution) were significantly decreased in individual Purkinje cells (Wilcoxon test; p = 0.011; n = 14; Figure 3D), confirming that intrinsic plasticity not only causes an overall shortening of ISIs, but specifically decreases the longest ISI (the pause) following the complex spike.

The observation that intrinsic plasticity affects pause duration as well as spike frequency leads to the question whether the phenomenon of pause shortening is simply a direct consequence of the enhanced number of spikes. Our analysis of pause and ISI values before and after tetanization does not support this possibility. Instead, we found that the change in pause duration is significantly larger than the change in ISI duration (pre-complex spike ISIs as a measure of excitability that is unaffected by the complex spike; p = 0.040; paired Student’s t test; Figures 3E and 3F). These data demonstrate that the pause and ISI duration are co-modulated, but show differences in the magnitude of modulation. This is in contrast to baseline conditions where the relation between pause and ISI (pre-complex spike) duration values can be described with good approximation by a linear regression (R^2: mean = 0.960, SD = 0.029; n = 10; p < 0.01 for each cell; Figure 3G). On the basis of this observation, we calculated the ratio of the pause duration and the ISI duration

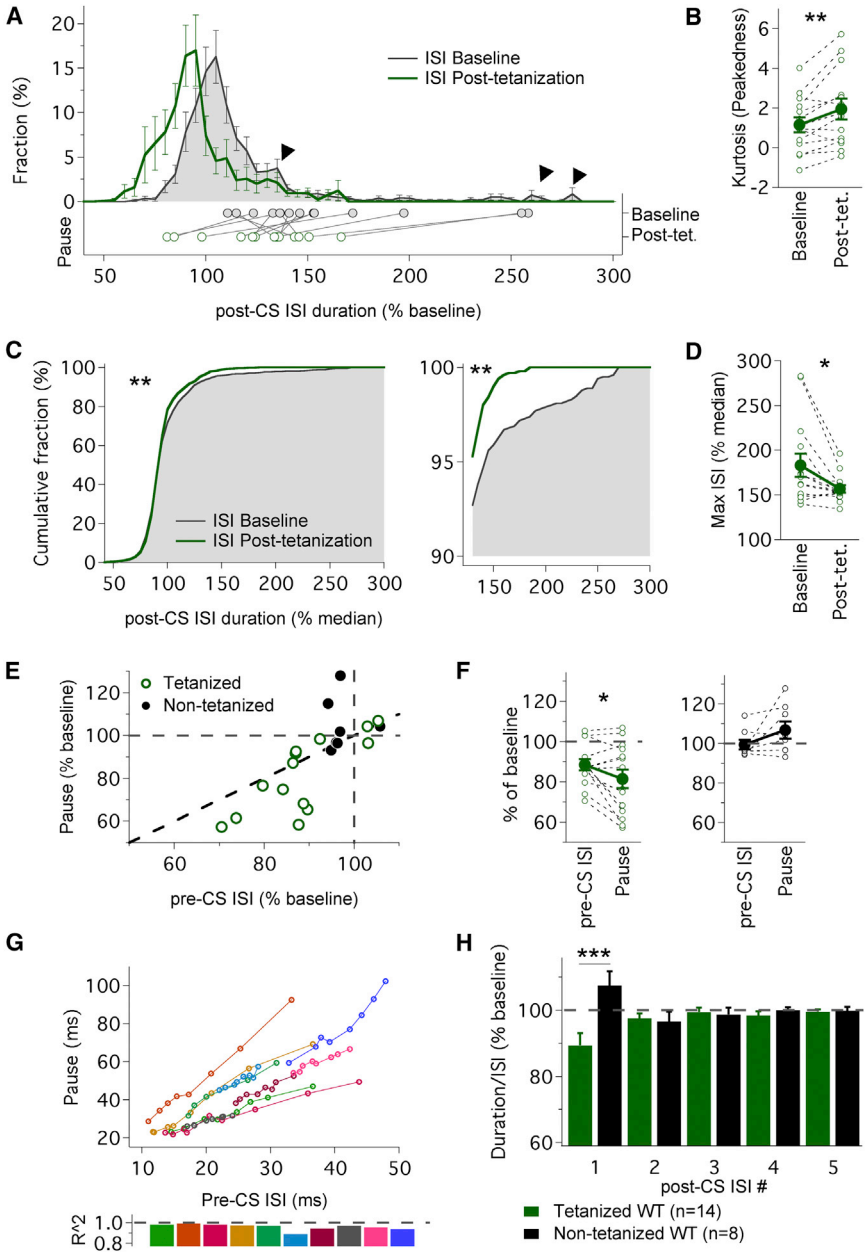

Figure 3. Intrinsic Plasticity Has a Larger Effect on the Pause Than on General Excitability

(A) Average distribution of ISI values following the complex spike (post-CS) before (black line; shaded gray) and after (green line) application of the IP protocol. The ISI duration is normalized to pre-complex spike (pre-CS) ISI values monitored before tetanization. Arrowheads outline tails of the distribution affected by the IP protocol. The dots below indicate the averaged pause duration for each cell before (filled dots) and after tetanization (empty dots).

(B) Kurtosis values of post-CS ISI values from each cell and their group average before and after tetanization (n = 14; **p = 0.009, Wilcoxon sign-ranked test).

(C) Cumulative distribution of pooled post-CS ISI values before (black line; shaded gray) and after (green line) application of the IP protocol. The ISI values were rescaled (compared to the distribution in A) by normalization in each individual cell to median pre-CS ISI values, and monitored before (n = 1,095 ISIs) and after tetanization (n = 1,081 ISIs) to assess changes in the tails.

(D) Maximal ISIs obtained from each individual cell, normalized as in (C) (n = 14; *p = 0.011; Wilcoxon sign-ranked test).

(E) Changes in pause duration plotted against changes in pre-CS ISI values for tetanized (green; n = 14) and non-tetanized cells (black; n = 8); the gray dashed lines indicate a null variation after the protocol, and the black dashed line indicates equal variation in ISI and pause.

(F) Comparison between the variation in the median pre-CS ISI and the variation in the pause in tetanized (left) and control cells (right; n = 14; *p = 0.040, paired t test).

(G) Pause duration plotted against pre-CS ISI duration at increasing amplitude of injected current (n = 10 cells); each line represents an individual cell, with 5–9 steps (single measurement) per cell.

(H) Intrinsic plasticity shortens the duration of the pause, but not the duration of subsequent ISIs (normalized values). Duration of the ISIs following the complex spike (pause = ISI #1) expressed as % of baseline after normalization to the average ISI (calculated from the eight ISIs preceding the complex spike). Only the pause was significantly shortened in tetanized cells (n = 14; compared to control cells, n = 8; repeated-measure ANOVA; group effect p = 0.0121, ISI effect p = 0.829, ISI × group interaction p = 0.00030; ***Tukey's post hoc comparisons: p = 0.000326, pause in tetanized versus non-tetanized cells).

The data shown in (A)–(F) and (H) were obtained from the same recordings that are shown in Figure 2B. Values are shown as mean ± SEM. *p < 0.05; **p < 0.01.

(pre-complex spike) and examined how this ratio is affected by the tetanization. We found that the normalized pause duration significantly decreased in the tetanized group (89.3% ± 3.7%; n = 14; no reduction occurred in the control group: 107.5% ± 4.3%; Figure 3H; SK2$^{-/-}$ group: 111.5% ± 5.0%, data not shown; Kruskal-Wallis comparison between groups: p = 0.0143), confirming a shortening of the pause duration after normalization to the ISI duration. This plasticity effect was specific to the pause (ISI #1 following the complex spike) as neither the ISI following the pause (ISI #2), nor ISIs #3–5 were significantly reduced after normalization to the average pre-complex spike ISI (Figure 3H). Together, these results demonstrate that pause plasticity is more than a mere consequence of enhanced spike frequency.

A prediction resulting from these data is that under experimental conditions where simple spike firing is suppressed, a component of pause plasticity should still be present. To test this prediction, we prevented simple spike activity by injection of hyperpolarizing bias currents and monitored the complex spike-evoked AHP—the cellular mechanism underlying the

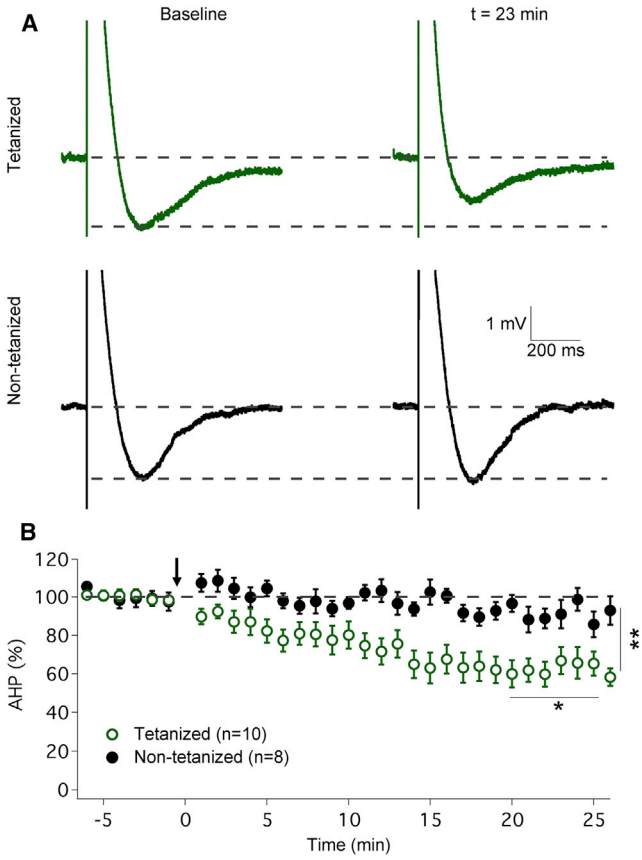

Figure 4. Intrinsic Plasticity Reduces the Amplitude of the Complex Spike AHP

(A) Typical traces showing complex spike AHPs before and after tetanization. The AHP amplitude is reduced in tetanized cells (top), but not in control cells (bottom).

(B) Time graph showing that the IP protocol reduces the AHP amplitude (n = 10), which remains unaltered in control cells (n = 8). The arrow indicates the time point of tetanization. Values are shown as mean ± SEM. *p < 0.05; **p < 0.01.

pause, and its correlate in the absence of simple spike firing—before and after tetanization. Application of the IP protocol (5 Hz, 7–8 s; pulses: 100 ms/500–700 pA) caused a significant reduction in AHP amplitudes (62.8% ± 6.3%; t = 19–25 min; n = 10; p = 0.0407; Figure 4) that was not observed in control cells (91.4% ± 4.6%; t = 19–25 min; n = 8; p = 0.0986; comparison between groups: p = 0.0077; Mann-Whitney U test). These data demonstrate a component of pause plasticity that can be isolated from spike rate plasticity and directly results from changes in the underlying pause mechanism itself. As SK2 channels play a role in both the complex spike AHP (Kakizawa et al., 2007) and the adjustment of spike frequency (Belmeguenai et al., 2010), it seems likely that intrinsic plasticity downregulates SK2 channels and that both pause plasticity and firing rate plasticity are related, but experimentally separable, consequences of SK2 channel modulation. The observation that under the experimental conditions used here (delayed baseline recording to stabilize pause measures) the mild remaining spike rate increase is not blocked in SK2$^{-/-}$ mice (Figure S1B), while pause plasticity is absent from these mice (Figure 2C), provides an additional example of such experimental separation.

DISCUSSION

Pause Plasticity Adjusts the Output Signal of the Cerebellar Cortex

A typical Purkinje cell spike pattern consists of a spike burst followed by a pause (Simpson et al., 1996). Purkinje cells are inhibitory projection neurons that provide the sole output of the cerebellar cortex (Eccles et al., 1967). In CbN target neurons that receive the GABAergic Purkinje cell terminals, a spike burst fired in a Purkinje cell causes inhibition, while the subsequent pause allows nuclei neurons to recover from the hyperpolarization by activation of rebound currents (for review, see Zheng and Raman, 2010). The rebound depolarization can trigger transient, enhanced spike firing (see also Alviña et al., 2008) that may even result in time-locked spiking in CbN neurons if activity in a sufficiently high number of Purkinje cells is synchronized (Person and Raman, 2012). In addition to the possible activation of CbN rebound firing, the sequence of hyperpolarization followed by rebound depolarization is essential for LTP induction at mossy fiber synapses onto CbN neurons (Pugh and Raman, 2006, 2009). Thus, rebound currents—permitted by Purkinje cell pauses—are crucial for spike coding and plasticity at the cerebellar output stage.

It has previously been suggested that changes in the duration of these pauses might play a role in cerebellar learning. LTD at PF synapses is accompanied by a shortening of pauses that follow PF bursts, and it was argued that the pause duration is the most reliable measure of learned PF patterns subsequent to LTD (Steuber et al., 2007). In this scenario, learned and familiar PF patterns result in shorter pauses than novel patterns, which consequently have a bigger impact on the output signal. Mechanistically, the link between LTD and pause plasticity may be provided by the calcium dependence of SK channels. In Purkinje cells, SK2 channels are activated by calcium influx through P/Q-type channels (Womack et al., 2004). It seems plausible that LTD lowers voltage-gated calcium influx, leading to a reduced activation of SK2 channels.

The findings presented here show that the same plasticity effect can be achieved through a direct modulation of SK2 channels in the absence of synaptic activation (non-synaptic induction protocol) and independent from synaptic plasticity (the protocol used does not trigger LTD or LTP; Belmeguenai et al., 2010). Thus, our study identifies a component of a cerebellar memory trace that rests entirely on intrinsic induction and expression mechanisms. This notion does not exclude the possibility that synaptic activation may trigger pause plasticity in the intact brain, as previously shown for intrinsic plasticity as measured by the spike frequency (Belmeguenai et al., 2010). Our recordings from SK2$^{-/-}$ Purkinje cells, complemented by pharmacological experiments (apamin), identify SK2 channel downregulation as the expression mechanism involved in pause plasticity. However, SK channel downregulation or blockade does not only reduce the AHP amplitude and pause duration, but also enhances the spike frequency in Purkinje cells (Edgerton and Reinhart, 2003; Belmeguenai et al., 2010). The additional

spikes will further shorten the pause. The observation that (1) a reduction in the amplitude of the AHP—the mechanism underlying the pause—can be observed when simple spike firing is suppressed, (2) the change in pause duration is significantly larger than the accompanying change in ISI duration, and (3) the change in pause duration remains significant after normalization to ISI values shows that pause plasticity is an aspect of intrinsic plasticity in Purkinje cells that is not just a consequence of the enhanced spike rate, but that rather a significant component of this plasticity phenomenon can be assigned to a reduction in the underlying AHP. In this scenario, both spike rate plasticity and pause plasticity represent potential consequences of an underlying SK2 channel modulation. Despite the shared mechanism, differences in plasticity magnitude may result from the non-linearity of spike generation and/or the particularly strong pause-related activation of SK channels by calcium influx during the complex spike (Schmolesky et al., 2002).

Pause Duration as a Plasticity Substrate in Fast-Firing Neurons

It has previously been pointed out that in Purkinje cells the duration of pauses following PF bursts more precisely reflects PF synaptic input weights than the number of evoked spikes or the spike latency (Steuber et al., 2007). In our study, we focus on complex spike pauses instead, because they are reliably observed and provide a predictable component of the extended complex spike waveform (Simpson et al., 1996). The CF input acts as an instructive signal in cerebellar plasticity (Piochon et al., 2012), and the interruption in simple spike firing that results from the complex spike-pause pattern is a well-characterized consequence of CF signaling (Simpson et al., 1996). Thus, regardless of synaptic origin a pause in spike firing is a signature component of the Purkinje cell output, and pause modulation is expected to have a major impact on downstream cerebellar signaling and to significantly contribute to a distributed cerebellar memory engram (for review, see Hansel et al., 2001; Gao et al., 2012). The notion that the pause duration plays a role in cerebellar information processing and learning is supported by the observation that pharmacological prolongation of post-complex spike pauses using 1-EBIO, a gating modulator of calcium-dependent K^+ channels, enhances the rate of cerebellar motor learning (Maiz et al., 2012).

Within the cerebellum, intrinsic plasticity has also been observed in granule cells (Armano et al., 2000) as well as in CbN neurons themselves (Aizenman and Linden, 2000).

CbN neurons spontaneously fire action potentials at elevated frequencies, just like Purkinje cells, but unlike cortical pyramidal neurons that show spontaneous discharge rates of $\leq$1 Hz (Margrie et al., 2002). Intrinsic plasticity seems to exist in different types of neurons regardless of their activity level at rest, but the specific roles assumed by forms of synaptic and non-synaptic plasticity, respectively, may differ depending on the spike firing behavior. While in pyramidal neurons, intrinsic plasticity will amplify signal processing (such as in EPSP-spike potentiation) and complement synaptic plasticity (Daoudal and Debanne, 2003; Magee and Johnston, 2005), its impact on spike firing will have a different quality in types of neurons that are spontaneously active and in which specific spike patterns, rather than the occurrence of individual spikes, determine the output signal. Pause plasticity in cerebellar Purkinje cells, as described here, provides an interesting example, because the activity-dependent reduction in pause duration modulates the signature output pattern generated by Purkinje cells. This characteristic spike burst-pause pattern is a direct consequence of the high tonic spike firing frequency in these neurons, which makes interruptions in spike firing a substrate for plasticity.

EXPERIMENTAL PROCEDURES

Patch-Clamp Recordings

Sagittal slices of the cerebellar vermis (200–300 μm) were prepared from P20-35 C57BL/6J mice after isoflurane anesthesia and decapitation. This procedure is in accordance with the guidelines of the Animal Care and Use Committee of the University of Chicago and the local committee for handling experimental animals of Kyoto University. In some experiments, $SK2^{-/-}$ mice (Bond et al., 2004) and WT littermates were used. Slices were cut on a vibratome (Leica VT1000S) using ceramic blades. The slices were kept at room temperature in artificial cerebrospinal fluid (ACSF) containing the following: 124 mM NaCl, 5 mM KCl, 1.25 mM Na_2HPO_4, 2 mM $MgSO_4$, 2 mM $CaCl_2$, 26 mM $NaHCO_3$, and 10 mM D-glucose, bubbled with 95% O_2 and 5% CO_2. Slices were allowed to recover for at least 1 hr and were then transferred to a submerged recording chamber superfused with ACSF at near-physiological temperature (32°C–34°C). The ACSF was supplemented with picrotoxin (100 μM) to block $GABA_A$ receptors. Whole-cell patch-clamp recordings were performed under visual control with differential interference contrast optics combined with near-infrared light illumination (IR-DIC) using a Zeiss AxioCam MRm camera and a ×40 IR-Achroplan objective, mounted on a Zeiss Axioscope 2FS microscope (Carl Zeiss MicroImaging). Patch pipettes (2.5–4 MΩ) were filled with internal saline containing the following: 9 mM KCl, 10 mM KOH, 120 mM K-gluconate, 3.48 mM $MgCl_2$, 10 mM HEPES, 4 mM NaCl, 4 mM Na_2ATP, 0.4 mM Na_3GTP, and 17.5 mM sucrose, with pH adjusted to 7.30 with KOH, and osmolarity adjusted to 300 mmol/kg with sucrose. Drugs were purchased from Sigma, Tocris, or R&D systems. Patch-clamp recordings were performed in current-clamp mode using an EPC-10 amplifier (HEKA Electronics). Membrane voltage and current were filtered at 3 kHz, digitized at 25 kHz, and acquired using Patchmaster software (HEKA Electronics). Membrane voltage was corrected for liquid junction potentials (11.7 mV). Access resistance was compensated (70%–80%) in current-clamp mode. Hyperpolarizing bias currents were applied to keep the membrane potential between −70 and −79 mV and to prevent spontaneous spike activity (−80 and −85 mV for the AHP recordings shown in Figure 4). In the Figure 1 experiments, Purkinje cell intrinsic excitability was monitored during the test periods by injection of brief (500 ms) depolarizing current pulses (100–200 pA every 20 s) adjusted to evoke ~10–20 spikes. For tetanization, depolarizing currents (100–200 pA; 100 ms) were injected at 5 Hz for 3 s. In the Figure 2 experiments, complex spike pauses were measured during the test periods by injection of 1-s-long depolarizing current pulses (150–700 pA every 30 s) adjusted to achieve a spike rate of 30–90 Hz to mimic tonic firing. A complex spike was elicited by CF stimulation after 500 ms (the traces displayed in Figure 2 zoom-in on the periods before and after the complex spike). For CF stimulation a glass pipette filled with ACSF was placed in the granule cell layer. For tetanization, depolarizing currents (500–700 pA; 100 ms) were applied at 5 Hz for 7–8 s. The complex spike pause was defined as the time between the complex spike onset (fast spike component) and the next subsequent simple spike. The spike frequency was calculated from the last eight ISIs preceding the CF stimulus. In all recordings, the input resistance (R_i) was measured by injection of hyperpolarizing test currents (−100 pA). Cells with a change in R_i or holding potential (V_h) of more than ~10% were excluded from the analysis.

Golgi Staining

Golgi staining was performed using a FD Rapid Golgi Stain Kit (FD NeuroTechnologies). Stained slices (135 μm) were imaged with a Zeiss AxioCam MRm

camera and a ×10 IR-Achroplan objective, mounted on a Zeiss Axioscope 2FS microscope (Carl Zeiss MicroImaging). Images were analyzed by NIH ImageJ software and NeuronJ plug-in software as previously described (Grasselli et al., 2011) to measure the total length of the dendritic arbor and the length of the primary dendrite. Sholl analysis of dendritic arbors was performed by the Sholl analysis plug-in in ImageJ, counting the number of intersections per radius step with increasing distance from the soma (5.5 μm starting radius; 5.5 μm radius steps).

Statistical Analysis

Data were analyzed using Fitmaster software (HEKA Electronics) and Igor Pro software (WaveMetrics). Statistical significance was determined by using the unpaired Student's t test for morphological analysis (Figure 1), the paired Student's t test (to test for significance of changes after an experimental manipulation in comparison to baseline), and the Mann-Whitney U test (between-group comparison), when appropriate. The paired Wilcoxon signed-rank test was used to examine changes in the median values of ISI distributions of individual cells (Figure 3A), Kurtosis values (Figure 3B), and maximum ISI values (Figure 3D). The Komogorov-Smirnov test was used to compare the distributions shown in Figure 3C. Kruskal-Wallis one-way ANOVA was used for a non-parametric multi-group comparison. Throughout the paper, all data are shown as mean ± SEM.

SUPPLEMENTAL INFORMATION

Supplemental Information includes Supplemental Experimental Procedures and two figures and can be found with this article online at http://dx.doi.org/10.1016/j.celrep.2016.02.054.

AUTHOR CONTRIBUTIONS

G.G., Q.H., G.O., and C.H. designed the experiments. G.G., Q.H., V.W., and G.O. performed the experiments and analyzed the data. J.P.A. provided the $SK2^{-/-}$ mice. G.G., J.P.A., and C.H. wrote the paper.

ACKNOWLEDGMENTS

We are grateful to Dr. Aaron Fox and members of the C.H. laboratory for feedback on the manuscript, Drs. Nicolas Brunel and Maurizio De Pittà for advice on statistical analysis, and Dr. Tomoo Hirano for providing a workstation and materials for some of the experiments. This study was supported by grants from the Kowa Foundation (to G.O.), from JSPS KAKENHI, Grant-in-Aid for Young Scientists (A) (26710002 to G.O.), and the National Institute of Neurological Disorders and Stroke (NS-062771 to C.H.).

Received: February 26, 2015
Revised: January 4, 2016
Accepted: February 8, 2016
Published: March 10, 2016

REFERENCES

Aizenman, C.D., and Linden, D.J. (2000). Rapid, synaptically driven increases in the intrinsic excitability of cerebellar deep nuclear neurons. Nat. Neurosci. *3*, 109–111.

Alviña, K., Walter, J.T., Kohn, A., Ellis-Davies, G., and Khodakhah, K. (2008). Questioning the role of rebound firing in the cerebellum. Nat. Neurosci. *11*, 1256–1258.

Armano, S., Rossi, P., Taglietti, V., and D'Angelo, E. (2000). Long-term potentiation of intrinsic excitability at the mossy fiber-granule cell synapse of rat cerebellum. J. Neurosci. *20*, 5208–5216.

Bell, C.C., and Grimm, R.J. (1969). Discharge properties of Purkinje cells recorded on single and double microelectrodes. J. Neurophysiol. *32*, 1044–1055.

Belmeguenai, A., Hosy, E., Bengtsson, F., Pedroarena, C.M., Piochon, C., Teuling, E., He, Q., Ohtsuki, G., De Jeu, M.T., Elgersma, Y., et al. (2010). Intrinsic plasticity complements long-term potentiation in parallel fiber input gain control in cerebellar Purkinje cells. J. Neurosci. *30*, 13630–13643.

Bloedel, J.R., and Roberts, W.J. (1971). Action of climbing fibers in cerebellar cortex of the cat. J. Neurophysiol. *34*, 17–31.

Bond, C.T., Herson, P.S., Strassmaier, T., Hammond, R., Stackman, R., Maylie, J., and Adelman, J.P. (2004). Small conductance Ca2+-activated K+ channel knock-out mice reveal the identity of calcium-dependent afterhyperpolarization currents. J. Neurosci. *24*, 5301–5306.

Cingolani, L.A., Gymnopoulos, M., Boccaccio, A., Stocker, M., and Pedarzani, P. (2002). Developmental regulation of small-conductance Ca2+-activated K+ channel expression and function in rat Purkinje neurons. J. Neurosci. *22*, 4456–4467.

Daoudal, G., and Debanne, D. (2003). Long-term plasticity of intrinsic excitability: learning rules and mechanisms. Learn. Mem. *10*, 456–465.

Eccles, J.C., Ito, M., and Szentagothai, J. (1967). The cerebellum as a neural machine (Berlin, Heidelberg, New York: Springer-Verlag).

Edgerton, J.R., and Reinhart, P.H. (2003). Distinct contributions of small and large conductance Ca2+-activated K+ channels to rat Purkinje neuron function. J. Physiol. *548*, 53–69.

Engbers, J.D., Anderson, D., Asmara, H., Rehak, R., Mehaffey, W.H., Hameed, S., McKay, B.E., Kruskic, M., Zamponi, G.W., and Turner, R.W. (2012). Intermediate conductance calcium-activated potassium channels modulate summation of parallel fiber input in cerebellar Purkinje cells. Proc. Natl. Acad. Sci. USA *109*, 2601–2606.

Gao, Z., van Beugen, B.J., and De Zeeuw, C.I. (2012). Distributed synergistic plasticity and cerebellar learning. Nat. Rev. Neurosci. *13*, 619–635.

Granit, R., and Phillips, C.G. (1956). Excitatory and inhibitory processes acting upon individual Purkinje cells of the cerebellum in cats. J. Physiol. *133*, 520–547.

Grasselli, G., Mandolesi, G., Strata, P., and Cesare, P. (2011). Impaired sprouting and axonal atrophy in cerebellar climbing fibres following in vivo silencing of the growth-associated protein GAP-43. PLoS ONE *6*, e20791.

Hansel, C., Linden, D.J., and D'Angelo, E. (2001). Beyond parallel fiber LTD: the diversity of synaptic and non-synaptic plasticity in the cerebellum. Nat. Neurosci. *4*, 467–475.

Häusser, M., and Clark, B.A. (1997). Tonic synaptic inhibition modulates neuronal output pattern and spatiotemporal synaptic integration. Neuron *19*, 665–678.

Kakizawa, S., Kishimoto, Y., Hashimoto, K., Miyazaki, T., Furutani, K., Shimizu, H., Fukaya, M., Nishi, M., Sakagami, H., Ikeda, A., et al. (2007). Junctophilin-mediated channel crosstalk essential for cerebellar synaptic plasticity. EMBO J. *26*, 1924–1933.

Magee, J.C., and Johnston, D. (2005). Plasticity of dendritic function. Curr. Opin. Neurobiol. *15*, 334–342.

Maiz, J., Karakossian, M.H., Pakaprot, N., Robleto, K., Thompson, R.F., and Otis, T.S. (2012). Prolonging the postcomplex spike pause speeds eyeblink conditioning. Proc. Natl. Acad. Sci. USA *109*, 16726–16730.

Margrie, T.W., Brecht, M., and Sakmann, B. (2002). In vivo, low-resistance, whole-cell recordings from neurons in the anaesthetized and awake mammalian brain. Pflugers Arch. *444*, 491–498.

Mathews, P.J., Lee, K.H., Peng, Z., Houser, C.R., and Otis, T.S. (2012). Effects of climbing fiber driven inhibition on Purkinje neuron spiking. J. Neurosci. *32*, 17988–17997.

Ohtsuki, G., Piochon, C., Adelman, J.P., and Hansel, C. (2012). SK2 channel modulation contributes to compartment-specific dendritic plasticity in cerebellar Purkinje cells. Neuron *75*, 108–120.

Person, A.L., and Raman, I.M. (2012). Purkinje neuron synchrony elicits time-locked spiking in the cerebellar nuclei. Nature *481*, 502–505.

Piochon, C., Kruskal, P., Maclean, J., and Hansel, C. (2012). Non-Hebbian spike-timing-dependent plasticity in cerebellar circuits. Front. Neural Circuits *6*, 124.

Pugh, J.R., and Raman, I.M. (2006). Potentiation of mossy fiber EPSCs in the cerebellar nuclei by NMDA receptor activation followed by postinhibitory rebound current. Neuron *51*, 113–123.

Pugh, J.R., and Raman, I.M. (2009). Nothing can be coincidence: synaptic inhibition and plasticity in the cerebellar nuclei. Trends Neurosci. *32*, 170–177.

Schmolesky, M.T., Weber, J.T., De Zeeuw, C.I., and Hansel, C. (2002). The making of a complex spike: ionic composition and plasticity. Ann. N Y Acad. Sci. *978*, 359–390.

Schreurs, B.G., Gusev, P.A., Tomsic, D., Alkon, D.L., and Shi, T. (1998). Intracellular correlates of acquisition and long-term memory of classical conditioning in Purkinje cell dendrites in slices of rabbit cerebellar lobule HVI. J. Neurosci. *18*, 5498–5507.

Simpson, J.I., Wylie, D.R., and De Zeeuw, C.I. (1996). On climbing fiber signals and their consequence(s). Behav. Brain Sci. *19*, 384–398.

Steuber, V., Mittmann, W., Hoebeek, F.E., Silver, R.A., De Zeeuw, C.I., Häusser, M., and De Schutter, E. (2007). Cerebellar LTD and pattern recognition by Purkinje cells. Neuron *54*, 121–136.

Womack, M.D., Chevez, C., and Khodakhah, K. (2004). Calcium-activated potassium channels are selectively coupled to P/Q-type calcium channels in cerebellar Purkinje neurons. J. Neurosci. *24*, 8818–8822.

Zhang, W., and Linden, D.J. (2003). The other side of the engram: experience-driven changes in neuronal intrinsic excitability. Nat. Rev. Neurosci. *4*, 885–900.

Zheng, N., and Raman, I.M. (2010). Synaptic inhibition, excitation, and plasticity in neurons of the cerebellar nuclei. Cerebellum *9*, 56–66.